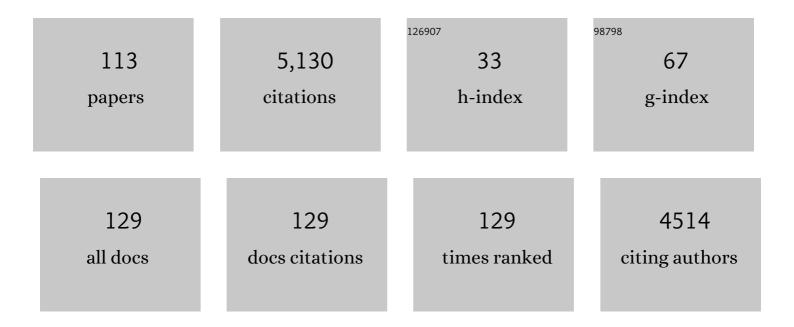
List of Publications by Year in descending order

Source: https://exaly.com/author-pdf/4763329/publications.pdf Version: 2024-02-01



#	Article	IF	CITATIONS
1	Automated Solution of Differential Equations by the Finite Element Method. Lecture Notes in Computational Science and Engineering, 2012, , .	0.3	1,283
2	Brain-wide glymphatic enhancement and clearance in humans assessed with MRI. JCI Insight, 2018, 3, .	5.0	290
3	Interstitial solute transport in 3D reconstructed neuropil occurs by diffusion rather than bulk flow. Proceedings of the National Academy of Sciences of the United States of America, 2017, 114, 9894-9899.	7.1	216
4	Preconditioning discretizations of systems of partial differential equations. Numerical Linear Algebra With Applications, 2011, 18, 1-40.	1.6	195
5	A Robust Finite Element Method for DarcyStokes Flow. SIAM Journal on Numerical Analysis, 2002, 40, 1605-1631.	2.3	188
6	Computation of Hemodynamics in the Circle of Willis. Stroke, 2007, 38, 2500-2505.	2.0	183
7	Sleep deprivation impairs molecular clearance from the human brain. Brain, 2021, 144, 863-874.	7.6	146
8	Direct numerical simulation of transitional flow in a patient-specific intracranial aneurysm. Journal of Biomechanics, 2011, 44, 2826-2832.	2.1	107
9	On the Computational Complexity of the Bidomain and the Monodomain Models of Electrophysiology. Annals of Biomedical Engineering, 2006, 34, 1088-1097.	2.5	96
10	Parameter-Robust Discretization and Preconditioning of Biot's Consolidation Model. SIAM Journal of Scientific Computing, 2017, 39, A1-A24.	2.8	94
11	Unified finite element discretizations of coupled Darcy–Stokes flow. Numerical Methods for Partial Differential Equations, 2009, 25, 311-326.	3.6	84
12	Real-World Variability in the Prediction of Intracranial Aneurysm Wall Shear Stress: The 2015 International Aneurysm CFD Challenge. Cardiovascular Engineering and Technology, 2018, 9, 544-564.	1.6	78
13	Multigrid Block Preconditioning for a Coupled System of Partial Differential Equations Modeling the Electrical Activity in the Heart. Computer Methods in Biomechanics and Biomedical Engineering, 2002, 5, 397-409.	1.6	73
14	Cerebrospinal fluid volumetric net flow rate and direction in idiopathic normal pressure hydrocephalus. NeuroImage: Clinical, 2018, 20, 731-741.	2.7	73
15	High-resolution CFD detects high-frequency velocity fluctuations in bifurcation, but not sidewall, aneurysms. Journal of Biomechanics, 2013, 46, 402-407.	2.1	71
16	Numerical methods for incompressible viscous flow. Advances in Water Resources, 2002, 25, 1125-1146.	3.8	70
17	Respiratory influence on cerebrospinal fluid flow – a computational study based on long-term intracranial pressure measurements. Scientific Reports, 2019, 9, 9732.	3.3	69
18	A Cell-Based Framework for Numerical Modeling of Electrical Conduction in Cardiac Tissue. Frontiers in Physics, 2017, 5, .	2.1	66

#	Article	IF	CITATIONS
19	A study of wall shear stress in 12 aneurysms with respect to different viscosity models and flow conditions. Journal of Biomechanics, 2013, 46, 2802-2808.	2.1	63
20	Intracranial pressure elevation alters CSF clearance pathways. Fluids and Barriers of the CNS, 2020, 17, 29.	5.0	53
21	CSF Flow Dynamics at the Craniovertebral Junction Studied with an Idealized Model of the Subarachnoid Space and Computational Flow Analysis. American Journal of Neuroradiology, 2010, 31, 185-192.	2.4	52
22	Uniform preconditioners for the time dependent Stokes problem. Numerische Mathematik, 2004, 98, 305-327.	1.9	51
23	Unified framework for finite element assembly. International Journal of Computational Science and Engineering, 2009, 4, 231.	0.5	51
24	Characterization of Cyclic CSF Flow in the Foramen Magnum and Upper Cervical Spinal Canal with MR Flow Imaging and Computational Fluid Dynamics. American Journal of Neuroradiology, 2010, 31, 997-1002.	2.4	51
25	Apparent diffusion coefficient estimates based on 24 hours tracer movement support glymphatic transport in human cerebral cortex. Scientific Reports, 2020, 10, 9176.	3.3	51
26	Sex differences in intracranial arterial bifurcations. Gender Medicine, 2010, 7, 149-155.	1.4	47
27	A Mixed Finite Element Method for Nearly Incompressible Multiple-Network Poroelasticity. SIAM Journal of Scientific Computing, 2019, 41, A722-A747.	2.8	45
28	An order optimal solver for the discretized bidomain equations. Numerical Linear Algebra With Applications, 2007, 14, 83-98.	1.6	44
29	Delayed clearance of cerebrospinal fluid tracer from choroid plexus in idiopathic normal pressure hydrocephalus. Journal of Cerebral Blood Flow and Metabolism, 2020, 40, 1849-1858.	4.3	43
30	The mechanisms behind perivascular fluid flow. PLoS ONE, 2020, 15, e0244442.	2.5	43
31	Patient-Specific 3D Simulation of Cyclic CSF Flow at the Craniocervical Region. American Journal of Neuroradiology, 2012, 33, 1756-1762.	2.4	38
32	Spinal Fluid Biomechanics and Imaging: An Update for Neuroradiologists. American Journal of Neuroradiology, 2014, 35, 1864-1869.	2.4	37
33	Flow characteristics in a canine aneurysm model: A comparison of 4D accelerated phaseâ€contrast MR measurements and computational fluid dynamics simulations. Medical Physics, 2011, 38, 6300-6312.	3.0	34
34	Non-invasive assessment of pulsatile intracranial pressure with phase-contrast magnetic resonance imaging. PLoS ONE, 2017, 12, e0188896.	2.5	34
35	Effect of Tonsillar Herniation on Cyclic CSF Flow Studied with Computational Flow Analysis. American Journal of Neuroradiology, 2011, 32, 1474-1481.	2.4	33
36	Numerical simulations of the pulsating flow of cerebrospinal fluid flow in the cervical spinal canal of Biomechanics, 2014, 47, 1082-1090.	2.1	33

#	Article	IF	CITATIONS
37	Variational data assimilation for transient blood flow simulations: Cerebral aneurysms as an illustrative example. International Journal for Numerical Methods in Biomedical Engineering, 2019, 35, e3152.	2.1	33
38	Poro-elastic modeling of Syringomyelia – a systematic study of the effects of pia mater, central canal, median fissure, white and gray matter on pressure wave propagation and fluid movement within the cervical spinal cord. Computer Methods in Biomechanics and Biomedical Engineering, 2016, 19, 686-698.	1.6	32
39	Orderâ€Optimal Preconditioners for Implicit Runge–Kutta Schemes Applied to Parabolic PDEs. SIAM Journal of Scientific Computing, 2007, 29, 361-375.	2.8	31
40	Direction and magnitude of cerebrospinal fluid flow vary substantially across central nervous system diseases. Fluids and Barriers of the CNS, 2021, 18, 16.	5.0	31
41	Transitional hemodynamics in intracranial aneurysms — Comparative velocity investigations with high resolution lattice Boltzmann simulations, normal resolution ANSYS simulations, and MR imaging. Medical Physics, 2016, 43, 6186-6198.	3.0	30
42	On the efficiency of symbolic computations combined with code generation for finite element methods. ACM Transactions on Mathematical Software, 2010, 37, 1-26.	2.9	26
43	Preconditioners for Saddle Point Systems with Trace Constraints Coupling 2D and 1D Domains. SIAM Journal of Scientific Computing, 2016, 38, B962-B987.	2.8	24
44	How does the presence of neural probes affect extracellular potentials?. Journal of Neural Engineering, 2019, 16, 026030.	3.5	24
45	An observation on Korn's inequality for nonconforming finite element methods. Mathematics of Computation, 2005, 75, 1-7.	2.1	23
46	Introduction to Numerical Methods for Variational Problems. Texts in Computational Science and Engineering, 2019, , .	0.1	23
47	CSF Pressure and Velocity in Obstructions of the Subarachnoid Spaces. Neuroradiology Journal, 2013, 26, 218-226.	1.2	22
48	Transitional flow in intracranial aneurysms – A space and time refinement study below the Kolmogorov scales using Lattice Boltzmann Method. Computers and Fluids, 2016, 127, 36-46.	2.5	22
49	Weakly Imposed Symmetry and Robust Preconditioners for Biot's Consolidation Model. Computational Methods in Applied Mathematics, 2017, 17, 377-396.	0.8	21
50	Fluid dynamics in syringomyelia cavities: Effects of heart rate, CSF velocity, CSF velocity waveform and craniovertebral decompression. Neuroradiology Journal, 2018, 31, 482-489.	1.2	21
51	Laplacian Preconditioning of Elliptic PDEs: Localization of the Eigenvalues of the Discretized Operator. SIAM Journal on Numerical Analysis, 2019, 57, 1369-1394.	2.3	21
52	Preconditioning of fully implicit Runge-Kutta schemes for parabolic PDEs. Modeling, Identification and Control, 2006, 27, 109-123.	1.1	21
53	Multigrid Methods for Discrete Fractional Sobolev Spaces. SIAM Journal of Scientific Computing, 2019, 41, A948-A972.	2.8	20
54	A numerical investigation of intrathecal isobaric drug dispersion within the cervical subarachnoid space. PLoS ONE, 2017, 12, e0173680.	2.5	19

#	Article	IF	CITATIONS
55	A uniformly stable Fortin operator for the Taylor–Hood element. Numerische Mathematik, 2013, 123, 537-551.	1.9	18
56	Direct numerical simulation of transitional hydrodynamics of the cerebrospinal fluid in Chiari I malformation: The role of cranioâ€vertebral junction. International Journal for Numerical Methods in Biomedical Engineering, 2017, 33, e02853.	2.1	18
57	Multi-resolution Bayesian CMB component separation through Wiener filtering with a pseudo-inverse preconditioner. Astronomy and Astrophysics, 2019, 627, A98.	5.1	18
58	Analysis and Approximation of Mixed-Dimensional PDEs on 3D-1D Domains Coupled with Lagrange Multipliers. SIAM Journal on Numerical Analysis, 2021, 59, 558-582.	2.3	18
59	Simulating CSF Flow Dynamics in the Normal and the Chiari I Subarachnoid Space during Rest and Exertion. American Journal of Neuroradiology, 2013, 34, 41-45.	2.4	17
60	The association between the pulse pressure gradient at the cranio-cervical junction derived from phase-contrast magnetic resonance imaging and invasively measured pulsatile intracranial pressure in symptomatic patients with Chiari malformation type 1. Acta Neurochirurgica, 2016, 158, 2295-2304.	1.7	17
61	A FEniCS tutorial. Lecture Notes in Computational Science and Engineering, 2012, , 1-73.	0.3	17
62	Computational Investigation of Cerebrospinal Fluid Dynamics in the Posterior Cranial Fossa and Cervical Subarachnoid Space in Patients with Chiari I Malformation. PLoS ONE, 2016, 11, e0162938.	2.5	16
63	Robust preconditioners for PDE-constrained optimization with limited observations. BIT Numerical Mathematics, 2017, 57, 405-431.	2.0	16
64	Effect of craniovertebral decompression on CSF dynamics in Chiari malformation Type I studied with computational fluid dynamics. Journal of Neurosurgery: Spine, 2014, 21, 559-564.	1.7	15
65	A MULTI-LEVEL SOLVER FOR GAUSSIAN CONSTRAINED COSMIC MICROWAVE BACKGROUND REALIZATIONS. Astrophysical Journal, Supplement Series, 2014, 210, 24.	7.7	15
66	Variations in the cerebrospinal fluid dynamics of the American alligator (Alligator mississippiensis). Fluids and Barriers of the CNS, 2021, 18, 11.	5.0	14
67	Stability analysis of the inverse transmembrane potential problem in electrocardiography. Inverse Problems, 2010, 26, 105012.	2.0	13
68	Cerebrospinal fluid flow in adults. Handbook of Clinical Neurology / Edited By P J Vinken and G W Bruyn, 2016, 135, 591-601.	1.8	13
69	The myodural bridge of the American alligator (<i>Alligator mississippiensis</i>) alters CSF flow. Journal of Experimental Biology, 2020, 223, .	1.7	13
70	Using Python to Solve Partial Differential Equations. Computing in Science and Engineering, 2007, 9, 48-51.	1.2	12
71	Preconditioning trace coupled 3 <i>d</i> â€l <i>d</i> systems using fractional Laplacian. Numerical Methods for Partial Differential Equations, 2019, 35, 375-393.	3.6	12
72	On the singular Neumann problem in linear elasticity. Numerical Linear Algebra With Applications, 2019, 26, e2212.	1.6	12

#	Article	IF	CITATIONS
73	Robust Preconditioners for Perturbed Saddle-Point Problems and Conservative Discretizations of Biot's Equations Utilizing Total Pressure. SIAM Journal of Scientific Computing, 2021, 43, B961-B983.	2.8	12
74	Modeling Excitable Tissue. Simula SpringerBriefs on Computing, 2021, , .	1.7	11
75	Robustness of common hemodynamic indicators with respect to numerical resolution in 38 middle cerebral artery aneurysms. PLoS ONE, 2017, 12, e0177566.	2.5	11
76	Magnitude and direction of aqueductal cerebrospinal fluid flow: large variations in patients with intracranial aneurysms with or without a previous subarachnoid hemorrhage. Acta Neurochirurgica, 2019, 161, 247-256.	1.7	10
77	Robust preconditioning for coupled Stokes–Darcy problems with the Darcy problem in primal form. Computers and Mathematics With Applications, 2021, 91, 53-66.	2.7	10
78	Analysis of the Minimal Residual Method Applied to Ill Posed Optimality Systems. SIAM Journal of Scientific Computing, 2013, 35, A785-A814.	2.8	9
79	Estimation of CSF Flow Resistance in the Upper Cervical Spine. Neuroradiology Journal, 2013, 26, 106-110.	1.2	9
80	Numerical study of intrathecal drug delivery to a permeable spinal cord: effect of catheter position and angle. Computer Methods in Biomechanics and Biomedical Engineering, 2017, 20, 1599-1608.	1.6	9
81	Comparison of phase-contrast MR and flow simulations for the study of CSF dynamics in the cervical spine. Neuroradiology Journal, 2018, 31, 292-298.	1.2	9
82	Effect of the Central Canal in the Spinal Cord on Fluid Movement within the Cord. Neuroradiology Journal, 2013, 26, 585-590.	1.2	8
83	Accurate discretization of poroelasticity without Darcy stability. BIT Numerical Mathematics, 2021, 61, 941-976.	2.0	8
84	Efficient Preconditioners for Optimality Systems Arising in Connection with Inverse Problems. SIAM Journal on Control and Optimization, 2010, 48, 5143-5177.	2.1	7
85	CSF Flow in Chiari I and Syringomyelia from the Perspective of Computational Fluid Dynamics. Neuroradiology Journal, 2011, 24, 20-23.	1.2	6
86	Dynamics of a neuron–glia system: the occurrence of seizures and the influence of electroconvulsive stimuli. Journal of Computational Neuroscience, 2020, 48, 229-251.	1.0	6
87	Parameter Robust Preconditioning by Congruence for Multiple-Network Poroelasticity. SIAM Journal of Scientific Computing, 2021, 43, B984-B1007.	2.8	6
88	An observation on the uniform preconditioners for the mixed Darcy problem. Numerical Methods for Partial Differential Equations, 2020, 36, 1718-1734.	3.6	5
89	Solving the EMI Equations using Finite Element Methods. Simula SpringerBriefs on Computing, 2021, , 56-69.	1.7	5
90	Slope limiting the velocity field in a discontinuous Galerkin divergence-free two-phase flow solver. Computers and Fluids, 2020, 196, 104322.	2.5	4

#	Article	IF	CITATIONS
91	Sub-voxel Perfusion Modeling in Terms of Coupled 3d-1d Problem. Lecture Notes in Computational Science and Engineering, 2019, , 35-47.	0.3	4
92	Parameter-robust methods for the Biot–Stokes interfacial coupling without Lagrange multipliers. Journal of Computational Physics, 2022, 467, 111464.	3.8	4
93	Order optimal preconditioners for fully implicit Runge-Kutta schemes applied to the bidomain equations. Numerical Methods for Partial Differential Equations, 2011, 27, 1290-1312.	3.6	3
94	"Bucket―cerebrospinal fluid bulk flow: when the terrain disagrees with the map. Acta Neurochirurgica, 2019, 161, 259-261.	1.7	2
95	A Hybrid Approach to Efficient Finite-Element Code Development. Chapman & Hall/CRC Computational Science, 2007, , 391-420.	0.5	2
96	Iterative Solvers for EMI Models. Simula SpringerBriefs on Computing, 2021, , 70-86.	1.7	2
97	Improving Neural Simulations with the EMI Model. Simula SpringerBriefs on Computing, 2021, , 87-98.	1.7	2
98	Simulating epileptic seizures using the bidomain model. Scientific Reports, 2022, 12, .	3.3	2
99	Computational fluid dynamics evaluation of flow reversal treatment of giant basilar tip aneurysm. Interventional Neuroradiology, 2015, 21, 586-591.	1.1	1
100	Comparison of Aneurismal Hemodynamics Between 4-D Accelerated Phase-Contrast MR Angiography and Computational Fluid Dynamics Simulations: Initial Experience in a Canine Aneurysm Model. , 2010, , .		1
101	Robust Preconditioning and Error Estimates for Optimal Control of the Convection–DiffusionReaction Equation with Limited Observation in Isogeometric Analysis. SIAM Journal on Numerical Analysis, 2022, 60, 195-221.	2.3	1
102	Encoderâ€decoder neural networks for predicting future FTIR spectra – application to enzymatic protein hydrolysis. Journal of Biophotonics, 0, , .	2.3	1
103	Direct Numerical Simulation of Transitional Flow in a Patient-Specific MCA Aneurysm. , 2011, , .		Ο
104	On Non-Newtonian Effects in Cerebral Aneurysms: A Computational Study on 12 Patient Specific Aneurysms. , 2012, , .		0
105	Can ECG Recordings and Mathematics tell the Condition of Your Heart?. , 2010, , 287-319.		Ο
106	Construction of Preconditioners by Mapping Properties for Systems of Partial Differential Equations. , 2011, , 66-83.		0
107	Cerebrospinal Fluid Volumetric Net Flow Rate and Direction in Idiopathic Normal Pressure Hydrocephalus. SSRN Electronic Journal, 0, , .	0.4	0
108	Time-Dependent Variational Forms. Texts in Computational Science and Engineering, 2019, , 233-257.	0.1	0

#	Article	IF	CITATIONS
109	Variational Forms for Systems of PDEs. Texts in Computational Science and Engineering, 2019, , 259-280.	0.1	0
110	Variational Formulations with Finite Elements. Texts in Computational Science and Engineering, 2019, , 173-231.	0.1	0
111	Function Approximation by Global Functions. Texts in Computational Science and Engineering, 2019, , 7-68.	0.1	0
112	Physiological Background. , 0, , 1-19.		0
113	Reuse of standard preconditioners for higher-order time discretizations of parabolic PDEs. Journal of Numerical Mathematics, 2006, 14, 103-122.	3.5	0